

# Transthoracic echocardiography in the evaluation of pediatric pulmonary hypertension and ventricular dysfunction

Martin Koestenberger,<sup>1</sup> Mark K. Friedberg,<sup>2</sup> Eirik Nestaas,<sup>3</sup> Ina Michel-Behnke,<sup>4</sup> Georg Hansmann<sup>5</sup>

<sup>1</sup>Division of Pediatric Cardiology, Department of Pediatrics, Medical University Graz, Graz, Austria; <sup>2</sup>Labatt Family Heart Center, Hospital for Sick Children and University of Toronto, Toronto, Ontario, Canada; <sup>3</sup>Center for Cardiological Innovation, Department of Cardiology, Oslo University Hospital Rikshospitalet, Oslo, Norway; and Department of Paediatrics, Vestfold Hospital Trust, Vestfold, Norway; <sup>4</sup>Division of Pediatric Cardiology, Pediatric Heart Center Vienna, Department of Pediatrics and Adolescent Medicine, Medical University of Vienna, Vienna, Austria; <sup>5</sup>Department of Pediatric Cardiology and Critical Care, Hannover Medical School, Hannover, Germany

**Abstract:** Transthoracic echocardiography (TTE) is the most accessible noninvasive diagnostic procedure for the initial assessment of pediatric pulmonary hypertension (PH). This review focuses on principles and use of TTE to determine morphologic and functional parameters that are also useful for follow-up investigations in pediatric PH patients. A basic echocardiographic study of a patient with PH commonly includes the hemodynamic calculation of the systolic pulmonary artery pressure (PAP), the mean and diastolic PAP, the pulmonary artery acceleration time, and the presence of a pericardial effusion. A more detailed TTE investigation of the right ventricle (RV) includes assessment of its size and function. RV function can be evaluated by RV longitudinal systolic performance (e.g., tricuspid annular plane systolic excursion), the tricuspid regurgitation velocity/right ventricular outflow tract velocity time integral ratio, the fractional area change, tissue Doppler imaging–derived parameters, strain measurements, the systolic-to-diastolic duration ratio, the myocardial performance (Tei) index, the RV/left ventricle (LV) diameter ratio, the LV eccentricity index, determination of an enlarged right atrium and RV size, and RV volume determination by 3-dimensional echocardiography. Here, we discuss the potential use and limitations of TTE techniques in children with PH and/or ventricular dysfunction. We suggest a protocol for TTE assessment of PH and myocardial function that helps to identify PH patients and their response to pharmacotherapy. The outlined protocol focuses on the detailed assessment of the hypertensive RV; RV-LV crosstalk must be analyzed separately in the evaluation of different pathologies that account for pediatric PH.

**Keywords:** children, pulmonary hypertension, right ventricle.

*Pulm Circ* 2016;6(1):15-29. DOI: 10.1086/685051.

Pulmonary hypertension (PH) is a rare disease of the cardiopulmonary system that can be diagnosed at any age. PH can occur either as an idiopathic disease process (iPH) or secondary to other disease processes. Early evidence for the epidemiology of PH originated from adult registries; however, several newer pediatric international registries have contributed to our understanding of the disease in children as well.<sup>1-5</sup> Pediatric PH can be associated with a variety of underlying conditions, including congenital heart disease (CHD), connective-tissue disorders, pulmonary disease, and endocrine, metabolic, and infectious diseases such as HIV. PH is usually progressive from infancy to adulthood and associated with poor prognosis.<sup>4</sup> The recent World Symposium on Pulmonary Hypertension updated the clinical classification of PH to include several features related to pediatric PH.<sup>6</sup> In children, pulmonary arterial hypertension (PAH; i.e., group 1 PAH of the Nice classification of 2013<sup>6</sup>) is usually a severe, refractory, and lifelong disease. An international registry showed that about 57% of children had iPH, a proportion similar to that observed in adults.<sup>4,7</sup> PH associated with CHD (PH-CHD) is more frequent in children (36%) than in adults (10%),<sup>4</sup> while

other associated forms are uncommon in children.<sup>8</sup> For the initial assessment and follow-up of children with suspected or confirmed PH, transthoracic echocardiography (TTE) is the noninvasive diagnostic method of choice.<sup>5,9-11</sup> TTE allows a detailed description of cardiovascular anatomy, ventricular function, and flow determination and carries low risk and wider availability, compared with cardiac magnetic resonance imaging (MRI). The diagnostic accuracy for describing cardiac morphology is high, with a reported incidence of less than 100 errors in more than 50,000 echocardiograms.<sup>12</sup> With TTE,<sup>13</sup> and MRI as well,<sup>14</sup> the effects of growth (e.g., changes of age-dependent normal reference values) must be accounted for in the interpretation of different variables. Many functional variables were developed and validated for the assessment of the normal left ventricle (LV). However, normal right ventricle (RV) hemodynamic function is physiologically distinct from that of the LV, including differences in fiber arrangement,<sup>15</sup> lower RV afterload, and lower RV pressures, compared to the LV.

Here, we review the principles and applications of TTE in patients with PH. The pathophysiology of PH includes abnormal pres-

Address correspondence to Dr. Martin Koestenberger, Division of Pediatric Cardiology, Department of Pediatrics, Medical University Graz, Auenbruggerplatz 34/2, A-8036 Graz, Austria; e-mail: martin.koestenberger@medunigraz.at; or Dr. Georg Hansmann, Department of Pediatric Cardiology and Critical Care, Hannover Medical School, Hannover, Germany; e-mail: hansmann.georg@mh-hannover.de.

Submitted July 22, 2015; Accepted December 1, 2015; Electronically published January 14, 2016.

© 2016 by the Pulmonary Vascular Research Institute. All rights reserved. 2045-8932/2016/0601-0003. \$15.00.

sure elevation in the RV, leading to flattening of the interventricular septum, with the LV appearing D-shaped. The LV has reduced systolic and diastolic volumes but usually preserved global systolic function.<sup>16</sup> Although not the focus of this review, evaluation of the left heart, including LV systolic function (LV ejection fraction [EF], fractional shortening), longitudinal systolic LV function (mitral annular plane systolic excursion), and inflow and outflow Doppler of all valves, should be an integral part of the echocardiographic assessment of PH, to assess detrimental RV-LV interactions.<sup>17</sup> After the initial diagnostic evaluation for PAH, TTEs are usually performed at 6–12-month intervals and when there is a clinical change. TTE assessment of RV function is commonly known to be technically difficult in both children and adults. The anterior position of the RV in the chest limits TTE visualization. Moreover, the RV has a complex geometry, with a triangular shape in the sagittal plane and a more crescent shape in the coronal plane. The RV inflow and outflow tracts are difficult to image simultaneously with 2-dimensional (2D) and Doppler echocardiography. In the standard apical 4-chamber view, the RV is usually smaller than the LV. To optimize imaging of the RV lateral wall, the 4-chamber image may have to be modified. RV dimensions are best estimated from an RV-focused apical 4-chamber view,<sup>18</sup> although M-mode and 2D measurements of RV end-diastolic dimensions toward the outflow can be made in the parasternal views. From the apical position, to avoid underestimating the minor distance of the RV, the transducer is rotated rightward until the maximum diameter is obtained. To avoid overestimation, the transducer should be positioned over the cardiac apex, with the plane through the mid-LV. Care should be taken to obtain the maximum RV diameter without foreshortening the image. This can be accomplished by ensuring that the crux and apex of the heart are both visible. As part of its guidelines on chamber quantification, the American Society of Echocardiography (ASE) published recommendations for RV assessment in adults.<sup>18</sup> Practical recommendations and a proposed protocol on the use of TTE variables to assess PH are available for the adult population.<sup>9,19,20</sup> An echocardiographic study of a child with a suspected PH should include the assessment of the following variables: estimation of the systolic pulmonary artery pressure (PAP), by estimating right ventricular systolic pressure (RVSP) through the measurement of the maximal velocity of the tricuspid regurgitation (TR) jet by continuous-wave (CW) Doppler; estimation of mean PAP and end-diastolic PAP through CW Doppler velocity measurement of the pulmonary regurgitation (PR) jet in the parasternal short-axis (PSAX) view; RV longitudinal systolic function determination; RV strain and strain rate measurements; RV volume determination by 3-dimensional (3D) echocardiography; measurement of the RV systolic-to-diastolic duration ratio; determination of tissue Doppler velocities; measurement of the RV/LV diameter ratio and eccentricity index; and determination of the pulmonary artery (PA) acceleration time. The presence of a persistent ductus arteriosus (PDA) should be carefully evaluated in each child with PH so that the immediate or long-term option of PDA stenting in advanced pediatric pulmonary hypertensive vascular disease with near-systemic PAP is not missed (e.g., an “interventional ductal Potts shunt” procedure<sup>21,22</sup>).

However, interpretation of pediatric values is dependent on age and cardiac growth. Current pediatric recommendations will assist with this matter, although age- or body dimension-corrected z-scores are still lacking for many parameters.<sup>23</sup> Although recent studies supported the potential value of echocardiography as a tool in guiding management in children with PH,<sup>24,25</sup> there is still a knowledge gap in recommended use of TTE in pediatric PH patients.

Nevertheless, we aim to propose a pediatric imaging protocol for use of TTE for the initial diagnosis, follow-up, and treatment assessment of children with PH; a TTE study of a child with a suspected PH should include the assessment of all the variables shown in Table 1. The TTE variables, as well as their advantages and disadvantages, are shown in Tables 2 and 3.

## HEMODYNAMIC ASSESSMENT OF THE RV

### Estimation of PAP

**Systolic PAP.** The estimation of the systolic PAP (sPAP) is based on the peak velocity of the TR jet (TRV). The simplified Bernoulli equation using CW Doppler to assess the TRV (peak pressure;  $RVSP = sPAP = 4 \times (TRV)^2 + RA$  v-wave  $\approx 4 \times (TRV)^2 +$  mean RAP, where RA is right atrium and RAP is right atrial pressure) describes the relationship of TR and RVSP as a surrogate of sPAP in the absence of RV outflow tract (RVOT) obstruction, pulmonary valve stenosis, or PA stenosis. Other formulas, such as the linear regression-derived  $sPAP = 1.07 \times (4TRV + RAP) + 7.4$ ,

Table 1. TTE protocol in pediatric PH

| Variables to be assessed  |
|---|
| Estimation of the systolic PAP, through the TR jet velocity by CW Doppler     |
| Estimation of mean PAP and end-diastolic PAP through CW Doppler of the PR jet |
| Pulmonary artery acceleration time (PAAT)                                     |
| RV longitudinal systolic function (e.g., TAPSE)                               |
| RV fractional area change   |
| RV strain and strain rate measurements  |
| RV systolic to diastolic duration ratio by CW Doppler of the TR jet           |
| Tissue Doppler velocities (e.g., S')  |
| RV myocardial performance (Tei) index   |
| RV/LV diameter ratio  |
| Left ventricular eccentricity index (LV EI)                                   |
| RV and RA enlargement   |

Note: TTE alone is not sufficient to initiate a targeted therapy. CW: continuous-wave; LV: left ventricle; PAP: pulmonary artery pressure; PH: pulmonary hypertension; PR: pulmonary regurgitation; RA: right atrium; RV: right ventricle; S': peak systolic velocity; TAPSE: tricuspid annular plane systolic excursion; TR: tricuspid regurgitation; TTE: transthoracic echocardiography; 3D: 3-dimensional.

Table 2. Echocardiographic variables in suspected or confirmed pediatric PH

| Variables                      | Interpretation   | Initial      | Follow-up    |
|--------------------------------|--|--------------|--------------|
| Systolic PAP (sPAP), mmHg      | Bernoulli equation ( $dP = 4 \times TRV^2$ ); TRV used to estimate sPAP; sPAP > 50 mmHg at rest makes PH highly likely in adults         | Yes          | Yes          |
| Mean PAP (mPAP), mmHg          | Estimated mPAP = maximum PR velocity + mean RAP; pediatric PH defined as mPAP > 25 mmHg and PVRi > 3.0 WU m <sup>2</sup>                 | Yes          | Yes          |
| Diastolic PAP (dPAP), mmHg     | Estimated dPAP = minimal (end-diastolic) PR velocity + mRAP; dPAP is independent of RV stroke volume                                     | Yes          | Yes          |
| PAAT, ms                       | PAAT < 100 ms: high probability of PH in adults  | Yes          | Yes          |
| TAPSE, mm                      | Decreased in advanced PH with RV dysfunction in children   | Yes          | Yes          |
| RV FAC, %                      | Impaired RV FAC = decreased systolic RV function in adults   | Probably     | Probably     |
| Strain, %; SR, s <sup>-1</sup> | PH patients may have impaired longitudinal strain and strain rate at the RV free wall; strain and SR are frequently altered in severe PH | If available | If available |
| S/D ratio                      | Ratio > 1.4 inversely correlates with survival in children with PH   | Yes          | Probably     |
| TDI (S'), cm/s                 | Decreased in advanced adult and pediatric PH; impaired S' (measured in TDI, lateral RV wall) predicts adverse outcome                    | Yes          | Yes          |
| Tei index                      | Increased index predicts RV dysfunction in pediatric PH  | Yes          | Probably     |
| RV/LV ratio                    | RV/LV ratio > 1 = increased adverse-event risk in pediatric PH   | Yes          | Yes          |
| LV EI                          | LV EI > 1 in adult PH-impaired RVx of the pressure-loaded RV   | Yes          | Yes          |
| RV/RA dilation                 | RV and RA area increase in adult PH; pediatric data missing  | Yes          | Yes          |

Note: dP: pressure gradient; EI: eccentricity index; FAC: fractional area change; LV: left ventricle; PAAT: pulmonary artery acceleration time; PAP: pulmonary artery pressure; PH: pulmonary hypertension; PR: pulmonary regurgitation; PVRi: pulmonary vascular resistance index; RA: right atrium; RAP: right atrial pressure; RV: right ventricle; RVx: right ventricular function; S': peak systolic velocity; S/D ratio: systolic/diastolic duration ratio; SR: strain rate; TAPSE: tricuspid annular plane systolic excursion; TDI: tissue Doppler imaging; TR: tricuspid regurgitation; TRV: TR jet velocity; WU: Wood units.

could also be reliable when estimating echocardiographically determined sPAP in PH patients.<sup>26</sup> The RAP can be estimated on the basis of the diameter and respiratory variation of the inferior vena cava (IVC), although in pediatric clinical practice a value from 5 to 10 mmHg is mostly assumed. Usually, TRV values in adults above 3.4 m/s, corresponding to an sPAP > 50 mmHg at rest, indicate PH in adults with relatively high degree of certainty.

A limitation is that in cases with moderate to severe TR, the RVSP may be underestimated. Underestimation of the RVSP and therefore the sPAP may also occur because of a suboptimal Doppler insonation angle or an inadequate Doppler spectral envelope. Overestimation may occur because of measurement outside the modal velocity of the spectral envelope, overgaining the Doppler signal, or if pulmonary valve stenosis is present. In the presence of a ventricular septal defect with LV-to-RA shunts, sonographers should be careful to not misinterpret the LV-to-RA jet as a TR signal. Figure 1a demonstrates an example of increased TR jet velocity suggesting increased sPAP.

**Mean PAP and diastolic PAP.** If PR is measured with CW Doppler, then mean and diastolic PAP (mPAP and dPAP, respectively) can be estimated from the maximum (early-diastolic) and minimum (end-diastolic) PR velocity (PRV), respectively, with the simplified Bernoulli equation ( $mPAP = 4 \times$  (maximum diastolic

$PRV)^2 + RA \text{ v-wave} = 4 \times (PRV)^2 + \text{mean RAP}$ ;  $dPAP = 4 \times$  (maximum diastolic  $PRV)^2 + RA \text{ v-wave} = 4 \times$  (minimum end-diastolic  $PRV)^2 + mRAP$ ).<sup>27</sup> This enhances Doppler estimation of PAP and thus diagnosis of potential PAH, applying the accepted definition of pediatric PAH as mPAP > 25 mmHg with a pulmonary vascular resistance (PVR) index > 3.0 Wood units m<sup>2</sup> for biventricular circulations.<sup>28</sup> The mPAP and dPAP can be estimated, using CW Doppler of the PR jet in the PSAX view, by measurement of the peak and minimal diastolic velocities. Mean PAP and dPAP are not routinely used in the diagnosis and follow-up of pediatric PAH but may be useful when TR tracing is unreliable. Figure 1b shows an increased peak velocity of the PR jet and an increased end-diastolic velocity, showing an increased mPAP and dPAP. The mPAP is calculated as the PR gradient, with a markedly increased value of 48 mmHg compared to normal values (<25 mmHg). The pulmonary capillary wedge pressure (PCWP) can be estimated via the Nagueh formula ( $E/e'$ ) where  $e'$  is the average tissue Doppler imaging velocity of  $E'$  lateral and  $E'$  septum. Thus, the mean transpulmonary gradient can be estimated by determining the difference between mPAP estimated by PR jet (i.e., early-diastolic maximum velocity + mRAP) and the PCWP estimated by the Nagueh formula ( $E/e'$ ).<sup>29</sup>

A limitation of mPAP and dPAP estimations is that TR and PR velocities must be sampled from multiple views to assure the best envelope and maximal velocity. An overestimation of the RAP and

Table 3. Echocardiographic variables: advantages and disadvantages

| Variable            | Main advantages   | Main disadvantages   |
|---------------------|---|--|
| Systolic PAP (sPAP) | Easily to perform; is known to be of significant prognostic value for PH  | Depends of angle of CW Doppler interrogation; sPAP may be under/overestimated (severe TR)  |
| Mean PAP            | At times better angle via PR than via TR  | PR required for PR velocity measurements   |
| Diastolic PAP       | Independent of RV systolic function   | PR required for PR velocity measurements   |
| PAAT                | Can be measured in most of the patients; PH likely if PAAT < 100 ms   | Possible pulmonary valve artifacts; heart rate-dependent measure   |
| PE                  | Sign of heart failure   | No pediatric data available  |
| TAPSE               | Easily to perform; impaired RV function at values <2 SD of age-related values   | Does not take into account segmental or radial RV function and contractility   |
| FAC                 | Decreased FAC = impaired RV function  | High inter- and intraobserver variability  |
| Strain, strain rate | Regional deformation provides information on regional myocardial dysfunction; impaired RV longitudinal strain (<-12.5%) = greater PH severity | Relatively low temporal resolution that hinders tracking in the presence of high heart rates; strain and strain rate require a significant amount of postprocessing time |
| S/D ratio           | PH likely if S/D duration ratio > 1.4   | Requires presence of defined TR onset/end  |
| TDI (S')            | Easy to perform; decreased in adult and in pediatric PH patients  | Variability with different loading conditions, assessment of motion in a single dimension  |
| Tei index           | A combined ventricular-vascular index and independent of ventricular geometry   | Systolic and diastolic time interval in a single index, no distinction between systolic/diastolic dysfunction  |
| RV/LV ratio         | Easily obtained in the clinical setting; PH likely if ratio > 1   | Cannot be used in PH patients with significant left-to-right shunt lesions   |
| LV EI               | Adverse outcome in adult PH if LV EI > 1  | Off-axis images; maybe artificially flattened septum   |
| RV/RA measures      | Commonly used and simple; allows to indicate RV/RA enlargement  | Normative values in children only for RV, not RA; interatrial septal bowing may have an influence  |

Note: CW: continuous-wave; EI: eccentricity index; FAC: fractional area change; LV: left ventricle; PAAT: pulmonary artery acceleration time; PAP: pulmonary artery pressure; PE: pericardial effusion; PH: pulmonary hypertension; PR: pulmonary regurgitation; RA: right atrium; RV: right ventricle; S/D ratio: systolic/diastolic duration ratio; S', peak systolic velocity; TAPSE: tricuspid annular plane systolic excursion; TDI: tissue Doppler imaging; TR: tricuspid regurgitation.

the use of inadequate Doppler signals were also identified as frequent pitfalls in TTE that lead to incorrect assumption of PAP values.<sup>30</sup>

### PA acceleration time

PA acceleration time (PAAT) is the interval in milliseconds from the onset of ejection to the peak flow velocity and can be used for assessment of PVR.<sup>31</sup> The forward flow velocity profile, obtained in the PA just distal to the pulmonary valve, is used to obtain the PAAT.<sup>31</sup> In adults at risk for PAH, a PAAT of less than 100 ms indicates a high probability of increased PAP.<sup>32</sup> A PAAT > 100 ms suggests that there is no PAH, whereas a PAAT < 100 ms would increase the likelihood that PAH is present. The normal pulsed-wave (PW) Doppler profile in the RVOT is smooth, parabolic, and without "notching" of the Doppler envelope. A notch is associated with increased PVR among a cohort of adults with PAH.<sup>33</sup> In children, a PAAT > 120 ms was described to distinguish between PAH patients and healthy controls.<sup>34</sup> Figure 2 shows a short PAAT in a 9-year-old patient with PAH. For correct interpretation of PAAT,

correct placement of the cursor in the middle of the PA and accurate alignment along the PA long axis are essential.

Even when a TR signal is lacking, PAAT measurement is possible in 99% of patients, thereby providing an alternative estimation of PVR in adults.<sup>31</sup> The PAAT can also provide useful information that aids in the accuracy of PH diagnosis. Limitations of this method are that, in patients with left-to-right shunts, the PAAT should be interpreted carefully<sup>35</sup> and that absolute PAAT values are very much heart rate dependent; the ratio of PAAT to PA ejection time has therefore been proposed to correct for the shortening of ejection with higher heart rates.

### Presence of a pericardial effusion

The presence of a pericardial effusion (PE) is prognostic and indicates poorer survival in adult PAH patients.<sup>36</sup> The findings show that even a small amount of PE in an adult PAH patient portends poor prognosis.<sup>36</sup> PEs in adult PAH patients appear to relate to RV failure and evaluation of right-sided filling pressures, along with right atrial (RA) hypertension and increased pressure in the coronary si-

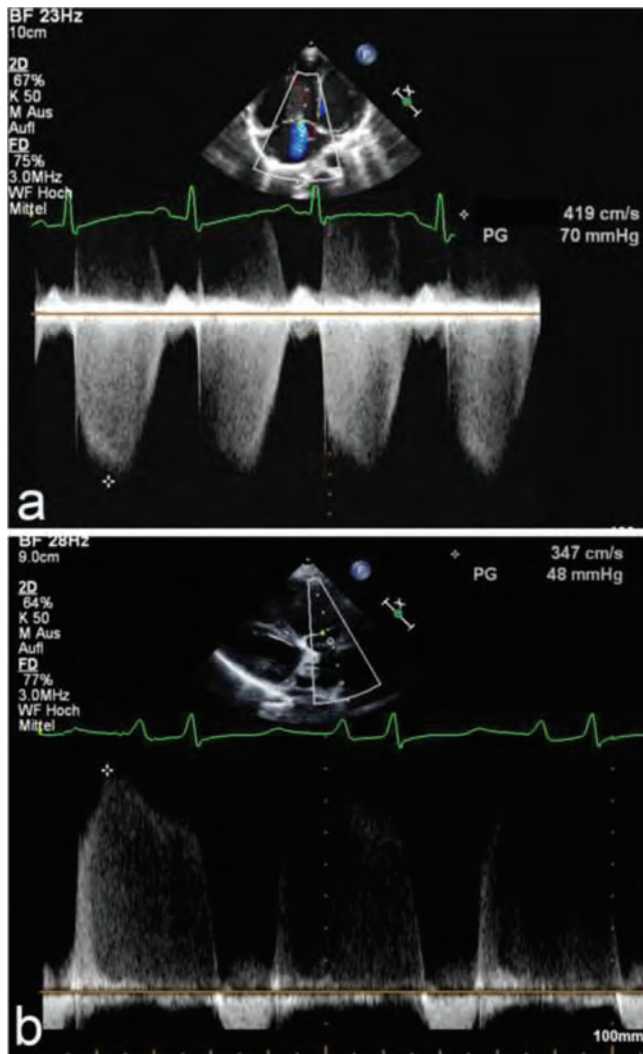


Figure 1. *a*, Apical 4-chamber view. Estimation of the systolic pulmonary artery pressure (PAP), by estimating the right ventricular systolic pressure by measurement of the velocity of the tricuspid regurgitation (TR) jet using continuous-wave (CW) Doppler. The dashed white line indicates CW Doppler cursor placement at the TR. The peak TR jet velocity is above 4 m/s, thus indicating an increased pressure gradient between the right ventricle and the right atrium (RA). This, added to an assumed RA pressure, estimates the systolic PAP. *b*, Parasternal short-axis view. Estimation of the mean PAP through CW Doppler of the pulmonary regurgitation (PR) jet. The dashed white line indicates CW Doppler cursor placement at the PR. The mean PAP is calculated as the PR gradient, with a markedly increased value of 48 mmHg compared to normal values (<25 mmHg). The end-diastolic regurgitant velocity is 2.5 m/s. When added to an assumed RA pressure of 10 mmHg, this estimates a pulmonary artery diastolic pressure of 35 mmHg.

nus.<sup>37</sup> The appearance of a new moderate or larger PE has been shown to be associated with increased mortality in adults, whereas this did not hold true when only a small PE developed.<sup>38</sup> A limitation on the relevance of a PE is that there currently are not sufficient data on the prognostic significance of a PE in pediatric PH.

### TRV/RVOT velocity time integral (VTI) ratio

There is a trend toward widespread noninvasive assessment of PVR in clinical practice. As the PVR increases, earlier and enhanced reflections of the pressure-wave profile of the RVOT appear, along with substantial changes in the RVOT VTI.<sup>39-42</sup> The RVOT VTI can be obtained by placing a PW Doppler sample volume in the proximal RVOT just within the pulmonary valve when imaged from the PSAX view. Vlahos et al.<sup>43</sup> also reported an excellent correlation between TRV/RVOT VTI and PVR in adult patients with moderate to severe pulmonary vascular disease. An increase in PVR is followed by a decrease in the RVOT VTI.<sup>43</sup> In that study population about half of the patients were pediatric.<sup>43</sup> After this relationship, when sPAP increases in PAH patients, TRV will increase and RVOT VTI is expected to decrease. The TRV/RVOT VTI ratio has recently been shown to correlate well with PVR measured at catheterization in pediatric PH patients.<sup>44</sup> Pande et al.<sup>44</sup> showed that, in this pediatric cohort (mean age: 9.7 years), the TRV/RVOT VTI ratio value of 0.14 provided a sensitivity of 96% and a specificity of 93% for a PVR of 6 Wood units. Normative pediatric RVOT VTI values were recently published.<sup>45</sup> These normative RVOT VTI values will help to overcome the problem of the currently limited use of the TRV/RVOT VTI ratio in children.

A limitation of RVOT imaging by TTE is the result of a lack of fixed reference points to ensure optimization of the RVOT. Using the RVOT VTI as an estimate of pulmonary flow has the additional limitation that it assumes a circular geometry of the RVOT; this might be the case in healthy children, but it is not in pediatric or adult patients with PH.

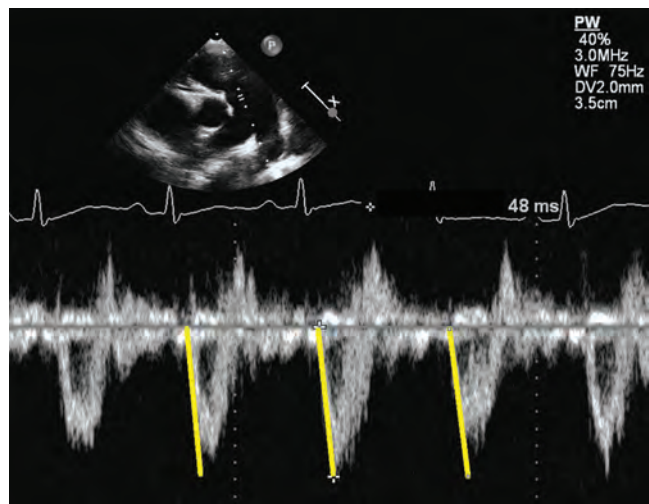


Figure 2. Parasternal short-axis view. Representative pulmonary artery flow velocity profile in the significantly enlarged main pulmonary artery of a 9-year-old patient with idiopathic pulmonary arterial hypertension. Note the rapid acceleration to peak flow velocity in early systole, marked by the yellow lines. Pulmonary artery acceleration time of 48 ms is reduced, compared to that of normal subjects.

## GLOBAL AND REGIONAL FUNCTIONAL ASSESSMENT OF THE RV

### RV longitudinal systolic function

Several indices for the assessment of longitudinal RV function are available, including the tricuspid annular plane systolic excursion (TAPSE).<sup>46</sup> TAPSE reflects longitudinal excursion of the tricuspid annulus toward the apex and is measured by M-mode from the 4-chamber view.<sup>47</sup> TAPSE changes with growth and increases from preterm infants to healthy adolescents.<sup>47,48</sup> Reference values of TAPSE measurements in adults and across the pediatric age range are available.<sup>49,50</sup> Recently published guidelines for the performance of a pediatric echocardiogram recommend TAPSE for the investigation of longitudinal RV function.<sup>23</sup> TAPSE is a reproducible index of RV systolic function in adult PH patients, and a reduced TAPSE has a high specificity for RV dysfunction.<sup>51</sup> A TAPSE of < 2 cm suggests that the RVEF is <40% in adults.<sup>52</sup> For every 1-mm decrease in TAPSE, the risk of death increases by 17% for adult PAH patients.<sup>51</sup> A significant amount of PH in childhood is CHD associated,<sup>53</sup> be it likely causally linked (large systemic left-to-right shunt) or out of proportion (e.g., severe PH in the setting of a small secundum atrial septal defect or left heart lesions). With sustained PH over years in children and young adults, TAPSE values decrease, progressively diverging from age-matched control values.<sup>54</sup> Thus, a decrease in TAPSE values may indicate a decline in RV systolic function. Figure 3 shows a significantly decreased TAPSE in a 12-year-old PH patient, with z-scores far below age-predicted values. A negative correlation was found between MRI-determined indexed RV end-diastolic volume (EDV) and TAPSE in patients with PH-CHD. The patients in this study suffered from PH-CHD after heart surgery in childhood and therefore show a difference from iPH patients.<sup>54</sup> In a prospective study of 66 treatment-naïve children with PH, the value of various clinical and echocardiographic measures in predicting transplant-free survival was examined and showed that treatment-induced changes in TAPSE were associated with improved survival.<sup>55</sup> TAPSE significantly improves after initiation or addition of PH therapy in pediatric PH patients.<sup>56</sup> A limitation of this method is that, although TAPSE appears to be a good indicator of global RV function, it does not take into account segmental RV dysfunction and contractility, such as decreased apical function. TAPSE also has a wide range of normal values.<sup>50</sup> Therefore, additional parameters should be combined with TAPSE for a more comprehensive and accurate assessment of RV systolic function.

### RV fractional area change

The RV fractional area change (FAC), representing the ratio of systolic area to diastolic area, is still a commonly used index of RV contraction. RV FAC is likely less reproducible than TAPSE but accounts for apical as well as basal function and for radial as well as longitudinal function, and it incorporates heart size.<sup>51</sup> Incomplete visualization of the RV cavity, which is more common in RV enlargement, has been shown to lead to a higher inter- and intraobserver variability.<sup>51</sup> In a recent pediatric PH study, FAC was correlated with indexed RV stroke work and TAPSE.<sup>57</sup> We believe that FAC

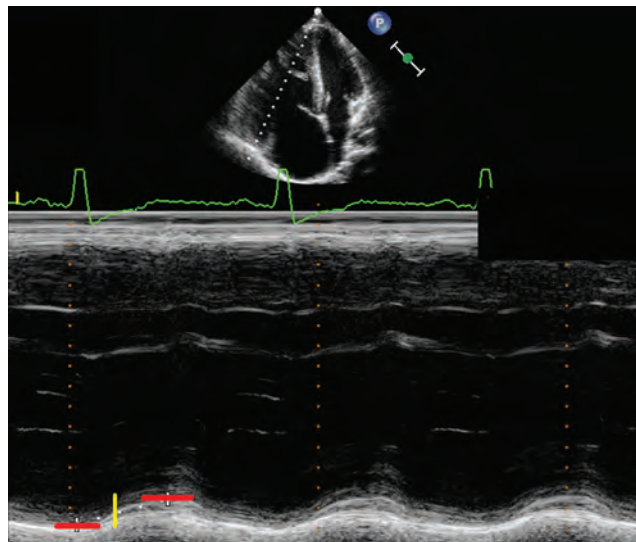


Figure 3. Apical 4-chamber view. The dotted white line indicates M-mode cursor placement at the tricuspid lateral annulus. Representative M-mode image of the tricuspid annular plane systolic excursion (TAPSE) in a 17-year-old patient with pulmonary hypertension secondary to congenital heart disease with a decreased TAPSE. The dotted white line in the M-mode shows the decreased TAPSE value and flat course of the excursion. The red lines mark the upper and lower borders of systolic motion, and the yellow line marks the measured distance. Note the dilation of the right ventricular and atrial cavities.

should be combined with other parameters for the assessment of RV function in children with PAH. A limitation of this method is that, like any ejection-phase measurement, the RV FAC is dependent on loading conditions. Another limitation is the usually sub-optimal endocardial tracing of the anterior RV wall.<sup>51</sup>

### Deformation imaging (RV strain and strain rate)

Regional wall motion abnormalities are relatively common in PH patients. Strain and strain rate seem to be useful in detecting such abnormalities and can be calculated noninvasively in both the LV and the RV, providing information on regional myocardial deformation and hence dysfunction in a variety of clinical settings. Myocardial velocities and displacement are influenced by global cardiac translational motion and by motion in adjacent myocardial segments. This limitation can be overcome by myocardial strain imaging. Strain is expressed as the percentage change in length from the original length. Strain rate is the rate of deformation (per second). Changes in strain rate have been suggested to better reflect changes in contractility as they occur in early systole and are perhaps less influenced by loading conditions.<sup>58</sup> Strain rate imaging provides a tool to quantify regional RV dysfunction in adult patients with PAH and reveals a characteristic regional pattern of abnormal RV free-wall function (Fig. 4).<sup>59</sup> It has been shown in adults that the more severe the PH, the more impaired the end-systolic longitudinal strain in the RV free wall.<sup>60</sup> While

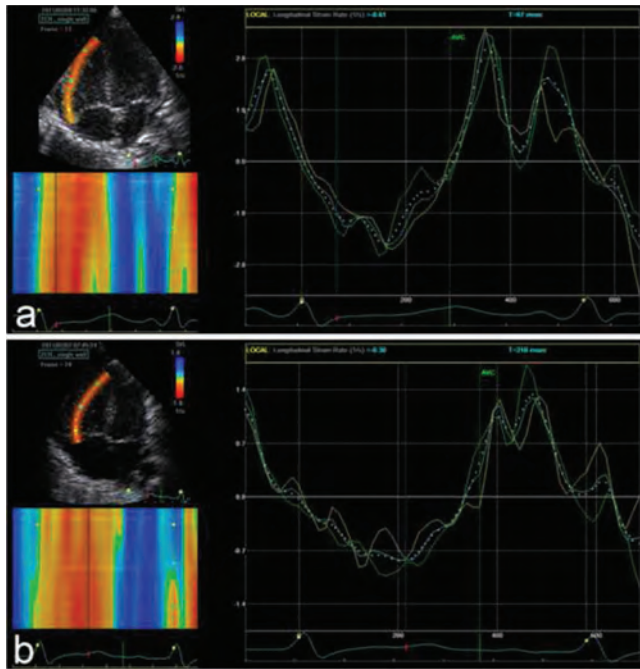


Figure 4. Apical 4-chamber view of the right lateral (free) wall. Strain rate by speckle tracking at day 1 of life in 2 neonates suffering from perinatal asphyxia and treated with hypothermia. *a*, From a neonate without pulmonary hypertension (PH); *b*, from a neonate suffering from PH (persistent PH of the newborn). One heart cycle is shown. Green curves are from apical segments, cyan curves from middle segments, yellow curves from basal segments, and dotted white curves represent the whole wall. Note that the peak values are lower in *b* (the neonate with PH) than in *a*, most evident for the peak systolic values.

RV strain reflects myocardial performance, it is influenced by increased afterload and will decrease with increasing RV afterload.<sup>61</sup> RV global longitudinal peak systolic strain and strain rate were significantly impaired in adults with PH, compared to controls,<sup>62</sup> with RV systolic strain most altered in patients with severe PH, when compared with patients with mild PH.<sup>62</sup> Significant correlations between RV strain and strain rate and mPAP were found in adult PAH patients.<sup>63</sup> The important value of serial measurement of RV systolic strain in the prediction of long-term prognosis was also shown in patients with PH.<sup>64</sup> An individual improvement of >5% in RV strain at follow-up correlated with better pulmonary hemodynamics, improved clinical status, and less clinical evidence of RV failure. An RV strain improvement of >5% may also predict greater long-term survival in PH patients.<sup>64</sup> This was also suggested in a small study in pediatric PH patients, where strain may be an earlier predictor of RV dysfunction than conventional measures, as well as revealing regional differences.<sup>65</sup>

Normative deformation values for healthy children are available.<sup>66</sup> Deformation imaging has also been performed in healthy and asphyxiated neonates.<sup>67-69</sup> Reduced longitudinal RV deformation has been shown in patients with congenitally corrected transposition of the great arteries suffering from increased RV afterload.<sup>70</sup> Dragulescu

and Mertens<sup>71</sup> showed that speckle-tracking techniques can be used in children to quantify longitudinal and circumferential strain.

The limitations of strain and strain rate measurements are the relatively low temporal resolution of 2D speckle tracking in the presence of high heart rates and the postprocessing time. Strain rate, in particular, results in inherently noisy signals and therefore low reproducibility. Consequently, at this time strain rate is a useful research tool (Fig. 5) but is not routinely used in clinical practice. Improving postprocessing times will probably result in a more routine application of strain rate in children.<sup>72</sup> Further study is needed to determine whether RV strain will provide a more sensitive tool to determine early or deteriorating RV dysfunction in pediatric PH.

### Systolic-to-diastolic duration ratio

The Doppler-derived ratio of systolic duration to diastolic duration (S/D) was initially described in 2006.<sup>73</sup> Heart rate is a major

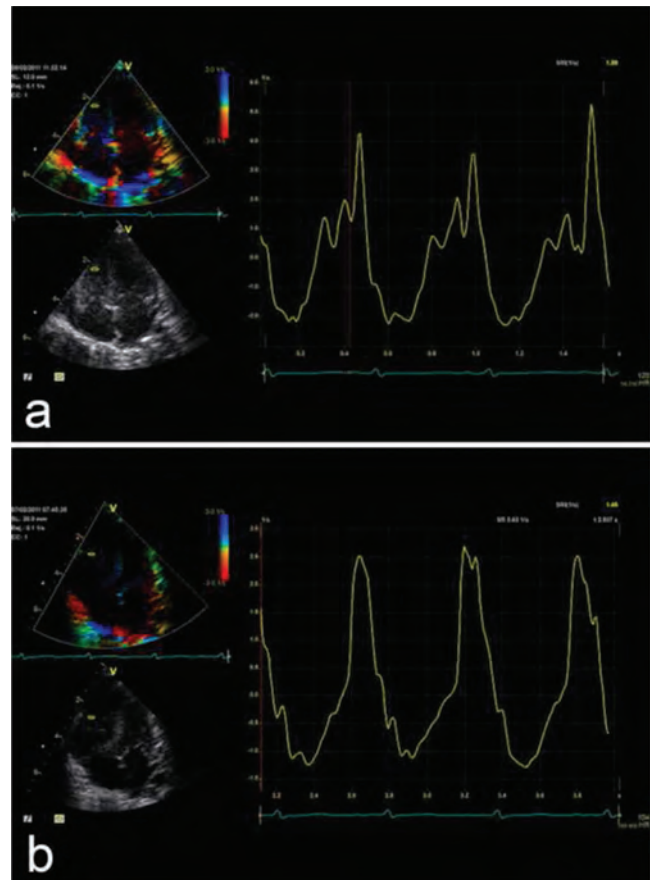


Figure 5. Apical 4-chamber view of the right lateral (free) wall. Strain rate by tissue Doppler imaging at day 1 of life in 2 neonates suffering from perinatal asphyxia and treated with hypothermia. Three heart cycles are shown. *a*, From a neonate without pulmonary hypertension (PH); *b*, from a neonate suffering from PH (persistent PH of the newborn). The curves show the value from a segment covering most of the right free wall. Note that the peak values are lower in *b* (the neonate with PH) than in *a*, most evident for the peak systolic values.

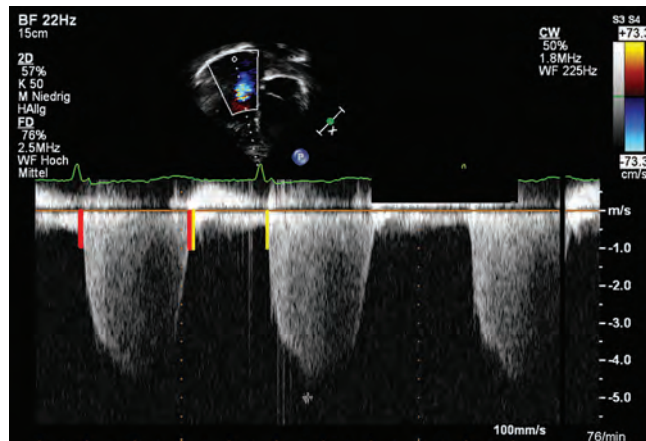


Figure 6. Apical 4-chamber view. Doppler-derived tricuspid regurgitation (TR) time interval ratio of systolic duration to diastolic duration (S/D). The S/D ratio was calculated by dividing the duration of the TR spectral Doppler flow pattern by the time interval of the cardiac cycle that did not include TR. Systolic and diastolic duration was measured, using TR duration, by continuous-wave Doppler from the apical 4-chamber view to calculate the S/D ratio. The red lines show the systolic duration, and the yellow lines mark the duration of diastole between the end and the onset of the TR signal within cardiac cycles.

determinant of systolic and diastolic duration, and at rest the former constitutes about 40% of the cardiac cycle duration in healthy children.<sup>74,75</sup> The S/D ratio is not dependent on heart size, which increases its worth and applicability in children. In children with PH, a significantly impaired S/D ratio was proposed as an indicator of RV dysfunction as well as adverse ventricular-ventricular interactions.<sup>76</sup> Children with significant PH have a marked decrease in diastolic duration and an increased S/D ratio, compared to control subjects, that progressively worsened with increasing heart rate.<sup>76</sup> An increased S/D ratio > 1.4 inversely correlated with survival in pediatric PH.<sup>76</sup> Figure 6 shows an increased S/D ratio in a 15-year-old adolescent with PH-CHD.

A limitation of the S/D ratio is that it requires the presence of clearly defined onset and end of TR on Doppler tracings. The S/D ratio is also influenced by heart rate and loading conditions. Although contraction is prolonged in PH, it is important to remember that ejection time is shortened in severe PH. Therefore, diastolic duration may be even shorter than systolic ejection time.<sup>77</sup>

### Tissue Doppler velocities

Tissue Doppler velocities can be used to assess regional myocardial function. In the normal RV, there is predominantly longitudinal orientation of the RV myofibers, especially in the deeper layer, and consequently normal RV function is predominantly longitudinal. Longitudinal tissue Doppler imaging (TDI) velocities are therefore pertinent to assess systolic and diastolic RV function. Good correlations between systolic velocities and RVEF were found in an adult population that included patients with CHD.<sup>78</sup> Normal pediatric TDI data have been published.<sup>79-81</sup> Tissue velocities vary with

age and heart rate and correlate with cardiac growth;<sup>82</sup> therefore, tissue velocities are not independent of geometry—which has important implications in children with CHD, who have variable RV size, mass, and geometry. In healthy neonates born at or near term, the longitudinal systolic tricuspid annular peak velocity ( $S'$ ) was only 1.2 times the mitral annular velocity.<sup>83</sup> This differs from adults, in whom tricuspid annular velocity is much higher than mitral annular velocities. This difference may be the result of the increased afterload faced by the neonatal RV, compared to the adult RV. In adults, TDI measurements have been shown to have a sensitivity of only 33% and a specificity of 100% to identify patients with precapillary PAH and a negative predictive value of 85% to exclude precapillary PAH.<sup>84</sup> The  $S'$  has been demonstrated to be significantly reduced in adult PAH patients with reduced RV function.<sup>85</sup> In children with PH-CHD, the tricuspid annular  $S'$  has been shown to be significantly impaired.<sup>80</sup> RV TDI parameters such as  $S'$  correlate well with invasive pulmonary hemodynamics in pediatric PH-CHD patients and may therefore be useful for follow-up of these patients.<sup>86</sup> TDI velocities may also be useful markers of midterm outcomes in children with iPH.<sup>87</sup> Pediatric PH patients had lower  $S'$  and early-diastolic velocities ( $E'$ ) at the lateral tricuspid, septal, and lateral mitral walls, compared to controls.<sup>88</sup> These systolic and diastolic abnormalities may worsen with increasing age.<sup>89</sup> Figure 7 shows decreased  $S'$  values in a 16-year-old PH patient. TDI is applicable independent of chamber morphology and is not based on geometrical assumptions. The  $S'$  is suggested to be useful for serial assessment of RV systolic function in pediatric patients.<sup>90</sup> The limitations of TDI are predominantly related to dependence on loading conditions, assessment of myocardial motion in a single dimension, dependency on heart size, and the dependency on interrogation angle.

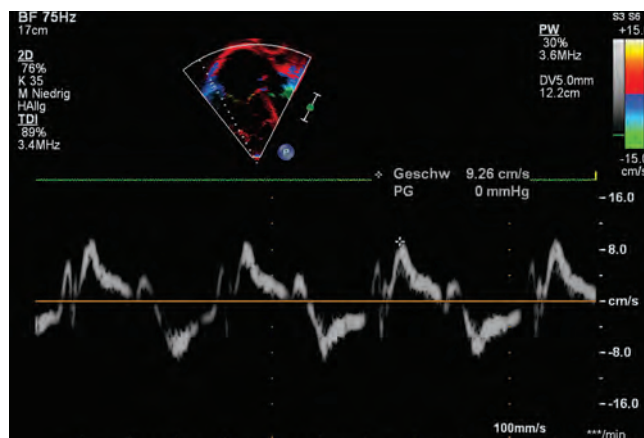


Figure 7. Apical 4-chamber view. Right ventricular (RV) tissue Doppler imaging (TDI) along the basal long axis of the RV free wall with the cursor through the lateral tricuspid annulus. Example of the pulsed-wave TDI-traced parameters tricuspid annular peak systolic velocity ( $S'$ ), peak early diastolic velocity ( $E'$ ), and peak late (atrial) diastolic velocity ( $A'$ ) in a 10-year-old patient with pulmonary hypertension secondary to congenital heart disease. Note the reduced values of every single parameter and the dilated right cavities.

### Myocardial performance index (Tei index)

The myocardial performance (Tei) index evaluates global ventricular function by measuring the ratio of isovolumic contraction and relaxation time intervals to ventricular ejection.<sup>91</sup> The longer the isovolumic phases, the higher the Tei index and the worse the RV performance. The Tei index has been reported to be important in the prediction of the outcome in children with heart failure and after repair of tetralogy of Fallot.<sup>92,93</sup> The RV Tei index has also been determined with TDI, allowing simultaneous measurement of systolic and diastolic velocities. The RV Tei index correlates well with right heart catheterization (RHC) parameters, including sPAP and mPAP, showing that it is influenced by loading conditions.<sup>94</sup> Children with PH have an increased Tei index compared to normal controls, more prominent in older children.<sup>89</sup> In children with PH, an increased Tei index is suggested to predict an RV dysfunction.<sup>95</sup> Figure 8 depicts the calculation of the Tei index in an 11-year-old patient with PH.

Advantages of the Tei index are that it is a combined ventricular-vascular index and can be measured independently of ventricular geometry. Its limitations include combination of systolic and diastolic time intervals, which does not allow distinction between systolic and diastolic dysfunction. With increased afterload, both isovolumic contraction and relaxation durations increase. Therefore, this index reflects increased RV afterload and not only RV dysfunction.

### VOLUMETRIC ASSESSMENT OF THE RV RV/LV diameter ratio

The RV/LV ratio was derived to combine a measure of RV size with septal shift secondary to elevated RV pressure. The RV/LV

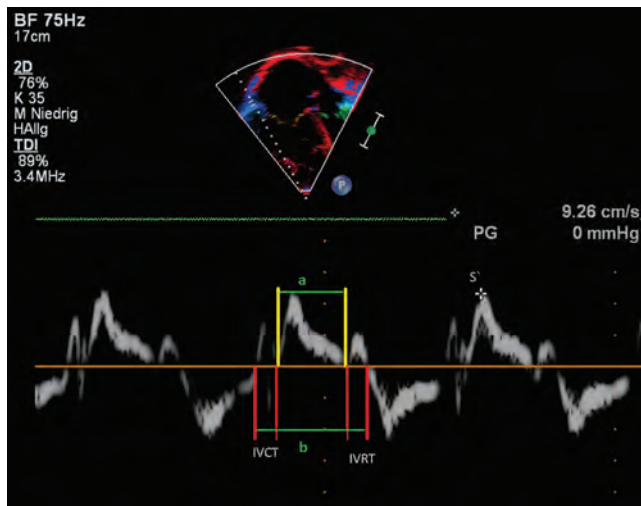


Figure 8. Right ventricular (RV) tissue Doppler imaging (TDI) along the basal long axis of the RV free wall in a 17-year-old adolescent with idiopathic pulmonary arterial hypertension. The longitudinal systolic shortening is labeled  $S'$  at 9.26 cm/s. RV myocardial performance (Tei) index can be obtained from the RV ejection time (green line marked "a") and from the isovolumic contraction time (IVCT) and isovolumic relaxation time (IVRT; red lines and green line marked "b").

ratio, measured in the PSAX view at the level of the papillary muscles at end-systole, is an index that has been shown to correlate well with invasive hemodynamic measures in children with PH.<sup>96</sup> The RV/LV ratio reflects the compression of the LV by the hypertensive RV and has been shown to be significantly higher in children with PH than in controls, and an RV/LV ratio  $> 1$  was associated with increased risk for adverse events in pediatric PH.<sup>96</sup>

The RV/LV end-systolic diameter (ESD) ratio can be easily obtained in the clinical setting and used for serial follow-up. Correct technique is important, as incorrect angulation can lead to under- or overestimation of ventricular diameters. This ratio is limited in patients with RV volume loading due to left-to-right shunt lesions or significant PR where RV size is increased only from volume loading.

### LV eccentricity index

In the pressure-loaded RV, septal flattening occurs in end-systole, resulting in an increased end-systolic LV eccentricity index (EI).<sup>97</sup> The LV EI is the ratio of the LV dimension in the minor axis parallel to the septum divided by the LV dimension in the minor axis perpendicular to the septum. Eccentricity index is determined in end-systole and end-diastole. An increased diastolic LV EI  $> 1$ , together with diastolic septal flattening, has been shown to predict adverse outcomes in adult idiopathic PAH (IPAH) patients, and this index is likely to be useful for stratification of prognosis in pediatric PH as well.<sup>98,99</sup> Figure 9 shows a significantly increased RV/LV ratio in a 13-year-old patient with PH-CHD. Limitations of this index are that slightly off-axis images may result in an artificially flattened septum, which may falsely increase the index, and that an inaccurate identification of the end-systole may influence the index.

### RV and LV diastolic function

PH is commonly associated with diastolic RV dysfunction that precedes the impairment of systolic RV function. In the apical 4-chamber view, a PW Doppler beam should be aligned as parallel as possible to RV inflow. The sample volume should be placed at the tip of the tricuspid leaflets.<sup>100</sup> The evaluation of RV diastolic function includes tricuspid inflow velocities ( $E$ ,  $A$ ,  $E/A$ ), TDI of the tricuspid annulus ( $E'$ ,  $A'$ , and  $E'/A'$ ), and deceleration time. The tricuspid  $E/E'$  ratio, RA area, and diastolic strain rate have promise in the evaluation of RV diastolic function. In adult studies with chronic heart failure and PH, the presence of RV diastolic dysfunction is associated with worse functional class and is an independent predictor of mortality.<sup>101</sup> In children with bronchopulmonary dysplasia, increasing tricuspid  $E/E'$  correlates with clinical severity of the disease.<sup>102</sup> In children with iPH, tricuspid valve  $E'$  correlates with mPAP and RV end-diastolic pressure.<sup>87</sup> In a recent study, diastolic parameters of RV in children with PH correlated with invasive measures of cardiac catheterization.<sup>103</sup>

Tricuspid inflow measures can be achieved with high reproducibility.<sup>104</sup> The presence of moderate to severe TR can confound measurements of the tricuspid inflow velocities and are excluded from most studies. In PH patients with advanced disease and evident RV-mediated impairment of LV filling, the late-diastolic LV filling pat-

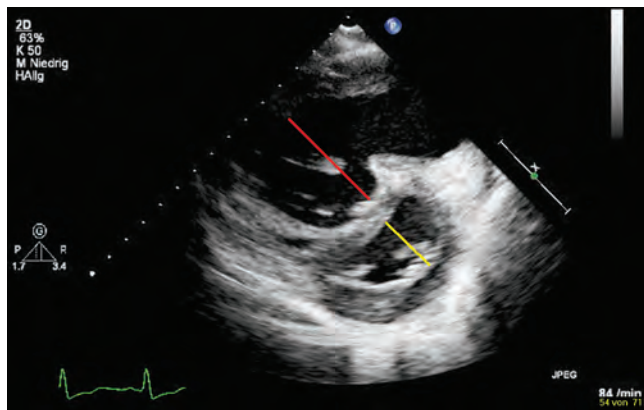


Figure 9. Parasternal short-axis view of the right ventricle (RV) and the left ventricle (LV): D-shaped LV and enlarged RV due to flattening of the interventricular septum. The end-systolic septal bowing is typical for pulmonary arterial hypertension (PAH). Remodeling of left and right cavities in a 14-year-old patient with severe idiopathic PAH. The RV/LV ratio was derived from RV and LV diameters at end-systole. The red line marks the severe dilation of the RV, with LV diameter (and compression) shown by the yellow line.

tern through the mitral valve will reverse, leading to  $E < A$ , and a short  $E$  deceleration time has been observed in adults.<sup>105</sup> The pulmonary venous Doppler flow can be abnormal in patients with LV diastolic dysfunction. In patients with PH from left-sided heart disease, the evaluation of mitral valve and pulmonary veins remains important in determining the cause of PH. Evaluation of LV systolic function can be measured by EF from biplane Simpson's formula<sup>106</sup> and the area-length method (Bullet) measuring LV end-diastolic diameter (EDD) and LVESD in the 4-chamber view and FAC in the PSAX view ( $LVEF = (LVEDV - LVESD) : LVEDD$ , where LV volumes are calculated monoplane as follows:  $LV \text{ volume} = 5/6 \times LV \text{ area SAX} \times LV \text{ length}$ ).<sup>107</sup>

### RV and RA enlargement

In adults, a basal RV diameter of  $>42$  mm and a midcavity diameter of  $>35$  mm have been shown to indicate RV dilation. Similarly, an end-diastolic length of  $>86$  mm indicates RV enlargement.<sup>18</sup> For the area of the RV, often the area divided by body surface area (the "indexed" area) is used. The ASE has published recommendations for quantification methods during the performance of a pediatric echocardiogram, with the RV internal-dimension parameters described as useful but with normative data for a comparison to dilated RVs still not available.<sup>23</sup> Recently, normative data of the pediatric RV internal dimensions have been published,<sup>108,109</sup> with sufficient TTE data of enlarged RV dimensions in pediatric PH currently missing. RV and RA enlargement, plus interatrial septal bowing from right to left (as shown in Fig. 10 in a 16-year-old adolescent with PH), indicates poor RV compliance, increased mean RAP, or both in adults.<sup>110</sup>

The measurement of RA dimensions, including RA diameter and area, in an apical 4-chamber view is a simple variable. An RA area  $> 20 \text{ cm}^2$  has been shown to be abnormal, and an RA area  $> 27 \text{ cm}^2$  showed a higher rate of death in adults with IPAH.<sup>110,111</sup>

In adult patients with chronic PAH, the RA size significantly increases and parallels signs of activation of the Frank-Starling mechanism in both right chambers. The RA size has been shown to be positively related to larger RV dimensions.<sup>112</sup> The IVC can be dilated in patients with PH because of rising RAP. It is measured in the subcostal longitudinal view with the IVC entering the RA. RAP can be estimated by IVC diameter and the presence of inspiratory collapse in adults.<sup>113,114</sup> An IVC diameter of  $<2$  cm that collapses by  $>50\%$  with a sniff suggests a normal RAP of 3 mmHg (range: 0–5 mmHg) in adults. An IVC diameter of  $>2$  cm that collapses by  $<50\%$  with a sniff suggests a high RAP of 15 mmHg (range: 10–20 mmHg).<sup>113,115</sup> In children, the IVC varies with age of the patient. Elevated RAP in children can be assessed by the percentage of collapse of the IVC during inspiration rather than by an absolute number. For the pediatric PH cohort, limited data for a comparison to a dilated RA are available, in contrast to RV size.<sup>109</sup> One of the major limitations of the reliability of RA and RV size determination is that only limited TTE data on RA and RV size enlargement in pediatric PH are available.

### 3D echocardiography

The most common 3D method of assessing RV volume in PH patients uses semiautomated border detection and a model of the RV that is used in semiautomated RV volume reconstruction.<sup>116,117</sup> Disk summation and apical rotational methods for RV volume and EF calculation have been shown to correlate well with MRI volume and EF in children<sup>118</sup> and adults.<sup>119</sup> RVEDV calculations of 3D data sets are available, with good correlations with other techniques, such as the MRI.<sup>120,121</sup> The lower reference limit for RVEF is 44%, from the disk summation method in adult patients. In a recent study by Kong et al.,<sup>122</sup> regional and global RV systolic dysfunction in adult PH patients measured by 3D echocardiography were inversely related to the pulmonary arterial systolic pressure and PVR. Normal values with this technique for RV size and function in adults

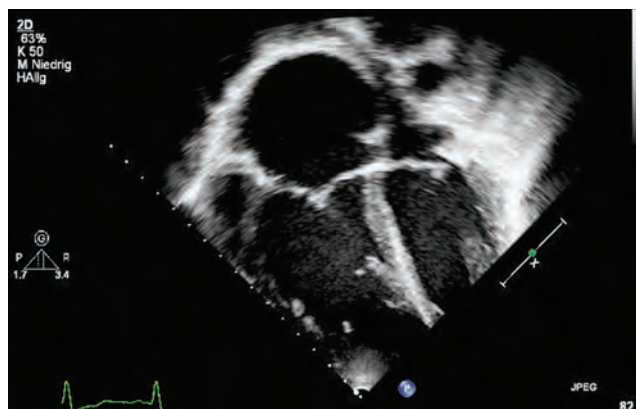


Figure 10. Apical 4-chamber view at ventricular end-systole, showing increased right atrial and right ventricular diameters. Typical echocardiographic feature in an 11-year-old patient with severe idiopathic pulmonary arterial hypertension with a dilation of the right atrium and right ventricle.

have been published.<sup>123</sup> Three-dimensional echocardiography outperformed 2D echocardiography in the assessment of RV volumes and compared favorably with cardiac MRI.<sup>124</sup> In adults with PAH, good correlation was found in the calculation of RVEF and RVEDV determined by either 3D echocardiography or MRI measurements.<sup>125</sup> It was recently shown that adult patients with some forms of PH had more dilated, hypertrophied, and poorly functioning RVs than adults with other forms.<sup>126</sup> The use of 3D echocardiography has been validated for the measurement of RV volumes and EF, which correlated well with those variables determined by MRI imaging in a pediatric population.<sup>127</sup> Validation of 3D echocardiographic assessment in children with complex CHD, including a small LV, has been performed,<sup>128</sup> while sufficient data in children with PH are scant. A limitation of this method is that 3D echocardiography is dependent on adequate acoustic windows, which had been appropriate in only about 50% of all patients,<sup>129</sup> because of inadequate image quality. Furthermore, an underestimation of the RV volume, when compared to MRI measurements, was reported from different groups that found the underestimation of RV volumes by 3D echocardiography mainly occurring in severely dilated RVs.<sup>119,130</sup>

## SUMMARY

In this review, we summarize the use of basic standard and more extended TTE variables in pediatric PH patients. TTE findings of suspected PH alone are not sufficient to establish the diagnosis of a pediatric PH and also not sufficient to initiate a specific therapy.<sup>1,131</sup> While important and mandatory for the initial confirmation of the diagnosis, a comprehensive RHC appears to be associated with a higher rate of complications in children than in adults and therefore requires specific expertise.<sup>1,132</sup> The use of TTE supports a goal-oriented “treat to target” therapy in adults and pediatric patients with PH.<sup>133</sup> Longitudinal investigations are of paramount importance in determining the effects of PH-specific therapies on growth and puberty in pediatric patients.<sup>134</sup> It is essential that TTE protocols for PH patients include assessment of RV hemodynamics, global and regional RV function, and RV volumetry. Although data on pediatric PH are still scant, we created a pediatric imaging protocol for use of TTE in the initial diagnosis, follow-up, and treatment of children with PH (Table 1) as our “best practices” for a TTE evaluation of children with various types of PH. The main focus of this review was on systolic RV function and size adaptation to increased RV afterload, but diastolic function changes must also be taken into consideration. Increased RA and RV surface areas, an altered EI, estimates of RAP from diastolic function indices, the RV Tei index, and several other variables are surrogate markers of diastolic RV function provided by TTE.<sup>135-137</sup> Echocardiographic 3D assessment of ventricular volumes and calculated RVEF and LVEF has made significant progress over the past decade, although it does not reach the accuracy of the gold-standard cardiac MRI.

More important than just measuring FAC, TAPSE, TDI, or other variables to assess RV function is properly performed investigation by the sonographer. Cardiac sonographers should become familiar with both traditional and newer techniques for more detailed assessments of ventricular performance in children with PH

and/or ventricular dysfunction.<sup>10</sup> Clinicians must develop an understanding of RV size and RV function measurements so that these can be integrated into clinical practice.

Regular and consistent usage of a TTE protocol may increase the identification of children with PH, leading to earlier comprehensive diagnosis and treatment. In concert with lab tests and exercise testing, these TTE variables are useful for the diagnostic workup and assessment of staging the disease in PH patients. A detailed TTE evaluation might reduce the cost of intensive and logistically demanding follow-up investigations such as cardiac MRI or cardiac catheterization, especially in the pediatric age group, in the future.

**Source of Support:** GH receives grant support from the German Research Foundation (DFG; HA 4348/2-1), Fördergemeinschaft deutsche Kinderherzzentren (W-H-001-2014), and Stiftung Kinderherz (2511-6-13-011).

**Conflict of Interest:** None declared.

## REFERENCES

1. Beghetti M, Berger RM, Schulze-Neick I, Day RW, Pulido T, Feinstein J, Barst RJ, Humpl T. Diagnostic evaluation of paediatric pulmonary hypertension in current clinical practice. *Eur Respir J* 2013;42(3):689-700.
2. McGoan MD, Miller DP. REVEAL: a contemporary US pulmonary arterial hypertension registry. *Eur Respir Rev* 2012;21(123):8-18. doi:10.1183/09059180.00008211.
3. Van Loon RL, Roofthoof MTR, Hillege HL, ten Harkel ADJ, van Osch-Gevers M, Delhaas T, Kapusta L, et al. Pediatric pulmonary hypertension in the Netherlands: epidemiology and characterization during the period 1991 to 2005. *Circulation* 2011;124(16):1755-1764.
4. Berger RMF, Beghetti M, Humpl T, Raskob GE, Ivy DD, Jing ZC, Bonnet D, Schulze-Neick I, Barst RJ. Clinical features of paediatric pulmonary hypertension: a registry study. *Lancet* 2012;379(9815):537-546.
5. Ploegstra MJ, Roofthoof MT, Douwes JM, Bartelds B, Elzenga NJ, van de Weerd D, Hillege HL, Berger RM. Echocardiography in pediatric pulmonary arterial hypertension: early study on assessing disease severity and predicting outcome. *Circ Cardiovasc Imaging* 2015;8:e000878. doi:10.1161/CIRCIMAGING.113.000878.
6. Simonneau G, Gatzoulis M, Adatia I, Celermajer D, Denton C, Ghofrani A, Gomez Sanchez MA, et al. Updated clinical classification of pulmonary hypertension. *J Am Coll Cardiol* 2013;62(25 suppl):D34-D41.
7. Badesch DB, Raskob GE, Elliott CG, Krichman AM, Farber HW, Frost AE, Barst RJ, et al. Pulmonary arterial hypertension: baseline characteristics from the REVEAL Registry. *Chest* 2010;137(2):376-387.
8. Schulze-Neick I, Beghetti M. Issues related to the management and therapy of paediatric pulmonary hypertension. *Eur Respir Rev* 2010;19(118):331-339. doi:10.1183/09059180.00008510.
9. Vonk Noordegraaf A, Haddad F, Bogaard HJ, Hassoun PM. Noninvasive imaging in the assessment of the cardiopulmonary vascular unit. *Circulation* 2015;131(10):899-913.
10. D'Alto M, Romeo E, Argiento P, Di Salvo G, Badagliacca R, Cirillo AP, Kaemmerer H, Bossone E, Naeije R. Pulmonary arterial hypertension: the key role of echocardiography. *Echocardiography* 2015;32(suppl. S1):S23-S37.
11. D'Alto M, Romeo E, Argiento P, D'Andrea A, Vanderpool R, Correra A, Bossone E, et al. Accuracy and precision of echocardiography versus right heart catheterization for the assessment of pulmonary hypertension. *Int J Cardiol* 2013;168(4):4058-4062.

12. Benavidez OJ, Gauvreau K, Jenkins KJ, Geva T. Diagnostic errors in pediatric echocardiography: development of taxonomy and identification of risk factors. *Circulation* 2008;117(23):2995–3001.
13. Koestenberger M, Friedberg MK, Ravekes W, Nestaas E, Hansmann G. Non-invasive imaging for congenital heart disease: recent innovations in transthoracic echocardiography. *J Clin Exp Cardiol* 2012;S8:002. doi:10.4172/2155-9880.S8-002.
14. Moledina S, Pandya B, Bartsota M, Mortensen KH, McMillan M, Quyam S, Taylor AM, Haworth SG, Schulze-Neick I, Muthurangu V. Prognostic significance of cardiac magnetic resonance imaging in children with pulmonary hypertension. *Circ Cardiovasc Imaging* 2013; 6(3):407–414.
15. Sheehan F, Redington A. The right ventricle: anatomy, physiology and clinical imaging. *Heart* 2008;94(11):1510–1515.
16. Bossone E, D'Andrea A, D'Alto M, Citro R, Argiento P, Ferrara F, Cittadini A, Rubenfire M, Naeije R. Echocardiography in pulmonary arterial hypertension: from diagnosis to prognosis. *J Am Soc Echocardiogr* 2013;26(1):1–14.
17. Friedberg MK, Redington AN. Right versus left ventricular failure: differences, similarities, and interactions. *Circulation* 2014;129(9): 1033–1044.
18. Rudski LG, Lai WW, Afilalo J, Hua L, Handschumacher MD, Chandrasekaran K, Solomon SD, Louie EK. Guidelines for the echocardiographic assessment of the right heart in adults: a report from the American Society of Echocardiography: endorsed by the European Association of Echocardiography, a registered branch of the European Society of Cardiology, and the Canadian Society of Echocardiography. *J Am Soc Echocardiogr* 2010;23(7):685–713.
19. Lancellotti P, Budts W, De Wolf D, Voigt JU, Pasquet A, De Sutter J, Friart A, Huez S, Paelinck B, Vachiéry JL. Practical recommendations on the use of echocardiography to assess pulmonary arterial hypertension—a Belgian expert consensus endorsed by the Working Group on Non-Invasive Cardiac Imaging. *Acta Cardiol* 2013;68(1): 59–69.
20. Badano LP, Gingham C, Easaw J, Muraru D, Grillo MT, Lancellotti P, Pinamonti B, et al. Right ventricle in pulmonary arterial hypertension: haemodynamics, structural changes, imaging, and proposal of a study protocol aimed to assess remodelling and treatment effects. *Eur J Echocardiogr* 2010;11(1):27–37.
21. Baruteau AE, Belli E, Boudjemline Y, Laux D, Lévy M, Simonneau G, Carotti A, Humbert M, Bonnet D. Palliative Potts shunt for the treatment of children with drug-refractory pulmonary arterial hypertension: updated data from the first 24 patients. *Eur J Cardiothorac Surg* 2015;47(3):e105–e110.
22. Latus H, Apitz C, Moysich A, Kerst G, Jux C, Bauer J, Schranz D. Creation of a functional Potts shunt by stenting the persistent arterial duct in newborns and infants with suprasystemic pulmonary hypertension of various etiologies. *J Heart Lung Transplant* 2014;33(5): 542–546.
23. Lopez L, Colan SD, Frommelt PC, Ensing GJ, Kendall K, Younoszai AK, Lai WW, Geva T. Recommendations for quantification methods during the performance of a pediatric echocardiogram: a report from the Pediatric Measurements Writing Group of the American Society of Echocardiography Pediatric and Congenital Heart Disease Council. *J Am Soc Echocardiogr* 2010;23(5):465–495.
24. Jone PN, Ivy DD. Echocardiography in pediatric pulmonary hypertension. *Front Pediatr* 2014;2:124. doi:10.3389/fped.2014.00124.
25. Espinola-Zavaleta N, Soto ME, Romero-Gonzalez A, Gómez-Puente LdC, Muñoz-Castellanos L, Gopal AS, Keirns C, Lupi-Herrera E. Prevalence of congenital heart disease and pulmonary hypertension in Down's syndrome: an echocardiographic study. *J Cardiovasc Ultrasound* 2015;23(2):72–77.
26. Pyxaras SA, Pinamonti B, Barbati G, Santangelo S, Valentincic M, Cettolo F, Secoli G, et al. Echocardiographic evaluation of systolic and mean pulmonary artery pressure in the follow-up of patients with pulmonary hypertension. *Eur J Echocardiogr* 2011;12(9):696–701.
27. Masuyama T, Kodama K, Kitabatake A, Sato H, Nanto S, Inoue M. Continuous-wave Doppler echocardiographic detection of pulmonary regurgitation and its application to noninvasive estimation of pulmonary artery pressure. *Circulation* 1986;74(3):484–492.
28. del Cerro MJ, Abman S, Diaz G, Freudenthal AH, Freudenthal F, Harikrishnan S, Haworth SG, et al. A consensus approach to the classification of pediatric pulmonary hypertensive vascular disease: report from the PVRI Pediatric Taskforce, Panama 2011. *Pulm Circ* 2011;1(2):286–298.
29. Nagueh SF, Mikati I, Kopelen HA, Middleton KJ, Quiñones MA, Zoghbi WA. Doppler estimation of left ventricular filling pressure in sinus tachycardia: a new application of tissue Doppler imaging. *Circulation* 1998;98(16):1644–1650.
30. Fisher MR, Forfia PR, Chamera E, Houston-Harris T, Champion HC, Girgis RE, Corretti MC, Hassoun PM. Accuracy of Doppler echocardiography in the hemodynamic assessment of pulmonary hypertension. *Am J Respir Crit Care Med* 2009;179(7):615–621.
31. Yared K, Noseworthy P, Weyman AE, McCabe E, Picard MH, Baggish AL. Pulmonary artery acceleration time provides an accurate estimate of systolic pulmonary arterial pressure during transthoracic echocardiography. *J Am Soc Echocardiogr* 2011;24(6):687–692.
32. Granstam SO, Björklund E, Wikström G, Roos MW. Use of echocardiographic pulmonary acceleration time and estimated vascular resistance for the evaluation of possible pulmonary hypertension. *Cardiovasc Ultrasound* 2013;11:7. doi:10.1186/1476-7120-11-7.
33. Arkles JS, Opatowsky AR, Ojeda J, Rogers F, Liu T, Prassana V, Marzec L, Palevsky HI, Ferrari VA, Forfia PR. Shape of the right ventricular Doppler envelope predicts hemodynamics and right heart function in pulmonary hypertension. *Am J Respir Crit Care Med* 2011;183(2):268–276.
34. Cevik A, Kula S, Olgunturk R, Tunaoglu FS, Oguz AD, Saylan B, Cilsal E, Sanli C. Assessment of pulmonary arterial hypertension and vascular resistance by measurements of the pulmonary arterial flow velocity curve in the absence of a measurable tricuspid regurgitant velocity in childhood congenital heart disease. *Pediatr Cardiol* 2013;34:646–655.
35. Matsuda M, Sekiguchi T, Sugishita Y, Kuwako K, Iida K, Ito I. Reliability of non-invasive estimates of pulmonary hypertension by pulsed Doppler echocardiography. *Br Heart J* 1986;56(2):158–164.
36. Fenstad ER, Le RJ, Sinak L, Maradit-Kremers H, Ammash NM, Ayalew A, Villarraga H, et al. Pericardial effusions in pulmonary arterial hypertension: characteristics, prognosis, and role of drainage. *Chest* 2013;144(5):1530–1538.
37. Natanzon A, Kronzon I. Pericardial and pleural effusions in congestive heart failure—anatomical, pathophysiologic, and clinical considerations. *Am J Med Sci* 2009;338(3):211–216.
38. Shimony A, Fox B, Langleben D, Rudski L. Incidence and significance of pericardial effusion in patients with pulmonary arterial hypertension. *Can J Cardiol* 2013;29(6):678–682.
39. Kouzu H, Nakatani S, Kyotani S, Kanzaki H, Nakanishi N, Kitakaze M. Noninvasive estimation of pulmonary vascular resistance by Doppler echocardiography in patients with pulmonary arterial hypertension. *Am J Cardiol* 2009;103(6):872–876.
40. Nakahata Y, Hiraishi S, Oowada N, Ando H, Kimura S, Furukawa S, Ogata S, Ishii M. Quantitative assessment of pulmonary vascular resistance and reactivity in children with pulmonary hypertension due to congenital heart disease using a noninvasive method: new Doppler-derived indexes. *Pediatr Cardiol* 2009;30(3):232–239.
41. Tonelli AR, Conci D, Tamarappoo BK, Newman J, Dweik RA. Prognostic value of echocardiographic changes in patients with pulmonary arterial hypertension receiving parenteral prostacyclin therapy. *J Am Soc Echocardiogr* 2014;27(4):733–741.
42. Abbas AE, Franey LM, Marwick T, Maeder MT, Kaye DM, Vlahos AP, Serra W, Al-Azizi K, Schiller NB, Lester SJ. Noninvasive assessment of

- pulmonary vascular resistance by Doppler echocardiography. *J Am Soc Echocardiogr* 2013;26(10):1170–1177.
43. Vlahos AP, Feinstein JA, Schiller NB, Silverman NH. Extension of Doppler-derived echocardiographic measures of pulmonary vascular resistance to patients with moderate or severe pulmonary vascular disease. *J Am Soc Echocardiogr* 2008;21(6):711–714.
  44. Pande A, Sarkar A, Ahmed I, Naveen Chandra G, Patil SK, Kundu CK, Arora R, Samanta A. Non-invasive estimation of pulmonary vascular resistance in patients of pulmonary hypertension in congenital heart disease with unobstructed pulmonary flow. *Ann Pediatr Cardiol* 2014;7(2):92–97.
  45. Koestenberger M, Nagel B, Ravekes W, Avian A, Burmas A, Grangl G, Cvirm G, Gamillscheg A. Right ventricular outflow tract velocity time integral determination in 570 healthy children and in 52 pediatric atrial septal defect patients. *Pediatr Cardiol* 2015;36(6):1129–1134.
  46. Miller D, Farah MG, Liner A, Fox K, Schluchter M, Hoit BD. The relation between quantitative right ventricular ejection fraction and indices of tricuspid annular motion and myocardial performance. *J Am Soc Echocardiogr* 2004;17(5):443–447.
  47. Koestenberger M, Nagel B, Ravekes W, Everett AD, Stueger H, Heinzl B, Sorantin E, Cvirm G, Fritsch P, Gamillscheg A. Systolic right ventricular function in pediatric and adolescent patients with tetralogy of Fallot: echocardiography versus magnetic resonance imaging. *J Am Soc Echocardiogr* 2011;24(1):45–52.
  48. Koestenberger M, Nagel B, Ravekes W, Urlesberger B, Raith W, Avian A, Halb V, Cvirm G, Fritsch P, Gamillscheg A. Systolic right ventricular function in preterm and term neonates: Reference values of the tricuspid annular plane systolic excursion (TAPSE) in 258 patients and calculation of Z-score values. *Neonatology* 2011;100(1):85–92.
  49. Lamia B, Teboul JL, Monnet X, Richard C, Chemla D. Relationship between the tricuspid annular plane systolic excursion and right and left ventricular function in critically ill patients. *Intensive Care Med* 2007;33(12):2143–2149.
  50. Koestenberger M, Ravekes W, Everett A, Stueger HP, Heinzl B, Gamillscheg A, Cvirm G, Boysen A, Fandl A, Nagel B. Right ventricular function in infants, children and adolescents: reference values of the tricuspid annular plane systolic excursion (TAPSE) in 640 healthy patients and calculation of z score values. *J Am Soc Echocardiogr* 2009;22(6):715–719.
  51. Forfia P, Fisher M, Mathai S, Houston-Harris T, Hemnes A, Borlaug B, Chamera E, et al. Tricuspid annular displacement predicts survival in pulmonary hypertension. *Am J Respir Crit Care Med* 2006;174(9):1034–1041.
  52. Lopez-Candales A, Rajagopalan N, Saxena N, Gulyasy B, Edelman K, Bazaz R. Right ventricular systolic function is not the sole determinant of tricuspid annular motion. *Am J Cardiol* 2006;98(7):973–977.
  53. Haworth SG, Hislop AA. Treatment and survival in children with pulmonary arterial hypertension: the UK pulmonary hypertension service for children 2001–2006. *Heart* 2009;95(4):312–317.
  54. Koestenberger M, Nagel B, Avian A, Ravekes W, Sorantin E, Cvirm G, Beran E, Halb V, Gamillscheg A. Systolic right ventricular function in children and young adults with pulmonary artery hypertension secondary to congenital heart disease and tetralogy of Fallot: tricuspid annular plane systolic excursion (TAPSE) and magnetic resonance imaging data. *Congenital Heart Dis* 2012;7(3):250–258.
  55. Ploegstra MJ, Douwes JM, Roofthoof MT, Zijlstra WM, Hillege HL, Berger RM. Identification of treatment goals in paediatric pulmonary arterial hypertension. *Eur Respir J* 2014;44(6):1616–1626.
  56. Bano M, Kanaan UB, Ehrlich AC, McCracken C, Morrow G, Oster ME, Sachdeva R. Improvement in tricuspid annular plane systolic excursion with pulmonary hypertension therapy in pediatric patients. *Echocardiography* 2015;32(8):1228–1232.
  57. Di Maria MV, Younoszai AK, Mertens L, Landeck BF II, Ivy DD, Hunter K, Friedberg MK. RV stroke work in children with pulmonary arterial hypertension: estimation based on invasive haemodynamic assessment and correlation with outcomes. *Heart* 2014;100(17):1342–1347.
  58. Ferferieva V, van den Bergh A, Claus P, Jasaityte R, Veulemans P, Pellens M, La Gerche A, Rademakers F, Herijgers P, D'hooge J. The relative value of strain and strain rate for defining intrinsic myocardial function. *Am J Physiol Heart Circ Physiol* 2012;302(1):H188–H195.
  59. Dambrauskaite, Delcroix M, Claus P, Herbots L, D'hooge J, Bijnens B, Rademakers F, Sutherland G. Regional right ventricular dysfunction in chronic pulmonary hypertension. *J Am Soc Echocardiograph* 2007;20(10):1172–1180.
  60. Puwanant S, Park M, Popović ZB, Tang WH, Farha S, George D, Sharp J, et al. Ventricular geometry, strain, and rotational mechanics in pulmonary hypertension. *Circulation* 2010;121(2):259–266.
  61. Kittipovanonth M, Bellavia D, Chandrasekaran K, Villarraga HR, Abraham TP, Pellikka PA. Doppler myocardial imaging for early detection of right ventricular dysfunction in patients with pulmonary hypertension. *J Am Soc Echocardiogr* 2008;21(9):1035–1041.
  62. Li Y, Xie M, Wang X, Lu Q, Fu M. Right ventricular regional and global systolic function is diminished in patients with pulmonary arterial hypertension: a 2-dimensional ultrasound speckle tracking echocardiography study. *Int J Cardiovasc Imaging* 2013;29(3):545–551.
  63. Naderi N, Ojaghi Haghghi Z, Amin A, Naghashzadeh F, Bakhshandeh H, Taghavi S, Maleki M. Utility of right ventricular strain imaging in predicting pulmonary vascular resistance in patients with pulmonary hypertension. *Congest Heart Fail* 2013;19(3):116–122.
  64. Hardegree EL, Sachdev A, Villarraga H, Frantz R, McGoon M, Kushwaha S, Hsiao J, et al. Role of serial quantitative assessment of right ventricular function by strain in pulmonary arterial hypertension. *Am J Cardiol* 2013;111(1):143–148.
  65. Okumura K, Humpl T, Dragulescu A, Mertens L, Friedberg MK. Longitudinal assessment of right ventricular myocardial strain in relation to transplant-free survival in children with idiopathic pulmonary hypertension. *J Am Soc Echocardiogr* 2014;27(12):1344–1351.
  66. Weidemann F, Eyskens B, Jamal F, Mertens L, Kowalski M, D'Hooge J, Bijnens B, et al. Quantification of regional left and right ventricular radial and longitudinal function in healthy children using ultrasound-based strain rate and strain imaging. *J Am Soc Echocardiogr* 2002;15(1):20–28.
  67. Joshi S, Edwards JM, Wilson DG, Wong JK, Kotecha S, Fraser AG. Reproducibility of myocardial velocity and deformation imaging in term and preterm infants. *Eur J Echocardiogr* 2010;11(1):44–50.
  68. Nestaas E, Støylen A, Brunvand L, Fugelseth D. Tissue Doppler derived longitudinal strain and strain rate during the first 3 days of life in healthy term neonates. *Pediatr Res* 2009;65(3):357–362.
  69. Nestaas E, Støylen A, Brunvand L, Fugelseth D. Longitudinal strain and strain rate by tissue Doppler are more sensitive indices than fractional shortening for assessing the reduced myocardial function in asphyxiated neonates. *Cardiol Young* 2011;21(1):1–7.
  70. Bos JM, Hagler DJ, Silvilairat S, Cabalka A, O'Leary P, Daniels O, Miller FA, Abraham TP. Right ventricular function in asymptomatic individuals with a systemic right ventricle. *J Am Soc Echocardiogr* 2006;19(8):1033–1037.
  71. Dragulescu A, Mertens LL. Developments in echocardiographic techniques for the evaluation of ventricular function in children. *Arch Cardiovasc Dis* 2010;103(11–12):603–614.
  72. Koopman LP, Slorach C, Hui W, Manlhiot C, McCrindle BW, Friedberg MK, Jaeggi ET, Mertens L. Comparison between different speckle tracking and color tissue Doppler techniques to measure global and regional myocardial deformation in children. *J Am Soc Echocardiogr* 2010;23(9):919–928.
  73. Friedberg MK, Silverman NH. Cardiac ventricular diastolic and systolic duration in children with heart failure secondary to idiopathic dilated cardiomyopathy. *Am J Cardiol* 2006;97(1):101–105.

74. Friedberg MK, Silverman NH. The systolic to diastolic duration ratio in children with hypoplastic left heart syndrome: a novel Doppler index of right ventricular function. *J Am Soc Echocardiogr* 2007;20(6):749–755.
75. Sarnari R, Kamal RY, Friedberg MK, Silverman NH. Doppler assessment of the ratio of the systolic to diastolic duration in normal children: relation to heart rate, age and body surface area. *J Am Soc Echocardiogr* 2009;22(8):928–932.
76. Alkon J, Humpl T, Manlihot C, McCrindle BW, Reyes J, Friedberg MK. Usefulness of the right ventricular systolic to diastolic duration ratio to predict functional capacity and survival in children with pulmonary arterial hypertension. *Am J Cardiol* 2010;106(3):430–436.
77. Rain S, Handoko ML, Trip P, Gan CT, Westerhof N, Stienen GJ, Paulus WJ, et al. Right ventricular diastolic impairment in patients with pulmonary arterial hypertension. *Circulation* 2013;128(18):2016–2025.
78. Wahl A, Praz F, Schwerzmann M, Bonel H, Koestner SC, Hullin R, Schmid JP, et al. Assessment of right ventricular systolic function: comparison between cardiac magnetic resonance derived ejection fraction and pulsed-wave tissue Doppler imaging of the tricuspid annulus. *Int J Cardiol* 2011;151(1):58–62.
79. Swaminathan S, Ferrer PL, Wolff GS, Gómez-Marín O, Rusconi PG. Usefulness of tissue Doppler echocardiography for evaluating ventricular function in children without heart disease. *Am J Cardiol* 2003;91(5):570–574.
80. Koestenberger M, Nagel B, Ravekes W, Avian A, Heinzl B, Fandl A, Rehak T, Sorantin E, Cvirn G, Gamillscheg A. Tricuspid annular peak systolic velocity (*S'*) in children and young adults with pulmonary artery hypertension secondary to congenital heart diseases, and in those with repaired tetralogy of Fallot: echocardiography and MRI data. *J Am Soc Echocardiogr* 2012;25(10):1041–1049.
81. Koestenberger M, Nagel B, Ravekes W, Avian A, Heinzl B, Cvirn G, Fritsch P, Fandl A, Rehak T, Gamillscheg A. Reference values of tricuspid annular peak systolic velocity in healthy pediatric patients, calculation of z score, and comparison to tricuspid annular plane systolic excursion. *Am J Cardiol* 2012;109(1):116–121.
82. Eidem BW, McMahon CJ, Cohen RR, Wu J, Finkelshteyn I, Kovalchin JP, Ayres NA, Bezold LI, O'Brian Smith E, Pignatelli RH. Impact of cardiac growth on Doppler tissue imaging velocities: a study in healthy children. *J Am Soc Echocardiogr* 2004;17(3):212–221.
83. Mori K, Nakagawa R, Nii M, Edagawa T, Takehara Y, Inoue M, Kuroda Y. Pulsed wave Doppler tissue echocardiography assessment of the long axis function of the right and left ventricles during the early neonatal period. *Heart* 2004;90(2):175–180.
84. Hammerstingl C, Schueler R, Bors L, Momcilovic D, Pabst S, Nickenig G, Skowasch D. Diagnostic value of echocardiography in the diagnosis of pulmonary hypertension. *PLoS ONE* 2012;7(6):e38519. doi:10.1371/journal.pone.0038519.
85. McLean AS, Ting I, Huang SJ, Wesley S. The use of the right ventricular diameter and tricuspid annular tissue Doppler velocity parameter to predict the presence of pulmonary hypertension. *Eur J Echocardiogr* 2007;8(2):128–136.
86. Cevik A, Kula S, Olgunturk R, Saylan B, Pektas A, Oguz D, Tunaoglu S. Doppler tissue imaging provides an estimate of pulmonary arterial pressure in children with pulmonary hypertension due to congenital intracardiac shunts. *Congenit Heart Dis* 2013;8(6):527–534.
87. Takatsuki S, Nakayama T, Jone PN, Wagner BD, Naoi K, Ivy DD, Saji T. Tissue Doppler imaging predicts adverse outcome in children with idiopathic pulmonary arterial hypertension. *J Pediatr* 2012;161(6):1126–1131.
88. Lammers AE, Haworth SG, Riley G, Maslin K, Diller GP, Marek J. Value of tissue Doppler echocardiography in children with pulmonary hypertension. *J Am Soc Echocardiogr* 2012;25(5):504–510.
89. Vorhies EE, Gajarski RJ, Yu S, Donohue JE, Fifer CG. Echocardiographic evaluation of ventricular function in children with pulmonary hypertension. *Pediatr Cardiol* 2014;35(5):759–766.
90. Pauliks L. Tissue Doppler myocardial velocity imaging in infants and children—a window into developmental changes of myocardial mechanics. *Echocardiography* 2013;30(4):439–446.
91. Tei C, Ling LH, Hodge DO, Bailey KR, Oh J, Rodeheffer RJ, Tajik AJ, Seward JB. New index of combined systolic and diastolic myocardial performance: a simple and reproducible measure of cardiac function: a study in normals and dilated cardiomyopathy. *J Cardiol* 1995;26(6):357–366.
92. Petko C, Minich LL, Everitt MD, Holubkov R, Shaddy RE, Tani LY. Echocardiographic evaluation of children with systemic ventricular dysfunction treated with carvedilol. *Pediatr Cardiol* 2010;31(6):780–784.
93. Yasuoka K, Harada K, Toyono M, Tamura M, Yamamoto F. Tei index determined by tissue Doppler imaging in patients with pulmonary regurgitation after repair of tetralogy of Fallot. *Pediatr Cardiol* 2004;25(2):131–136.
94. Vonk MC, Sander MH, van den Hoogen FH, van Riel PL, Verheugt FW, van Dijk AP. Right ventricle Tei-index: a tool to increase the accuracy of non-invasive detection of pulmonary arterial hypertension in connective tissue diseases. *Eur J Echocardiogr* 2007;8(5):317–321.
95. Cevik A, Kula S, Olgunturk R, Tunaoglu FS, Oguz AD, Pektas A, Saylan B. Quantitative evaluation of right ventricle function by thoracic echocardiography in childhood congenital heart disease patients with pulmonary hypertension. *Echocardiography* 2012;29(7):840–848.
96. Jone PN, Hinzman J, Wagner BD, Ivy DD, Younoszai A. Right ventricular to left ventricular diameter ratio at end-systole in evaluating outcomes in children with pulmonary hypertension. *J Am Soc Echocardiogr* 2014;27(2):172–178.
97. Ryan T, Petrovic O, Dillon JC, Feigenbaum H, Conley MJ, Armstrong WF. An echocardiographic index for separation of right ventricular volume and pressure overload. *J Am Coll Cardiol* 1985;5(4):918–927.
98. Ghio S, Klersy C, Magrini G, D'Armini AM, Scelsi L, Raineri C, Pasotti M, Serio A, Campana C, Viganò M. Prognostic relevance of the echocardiographic assessment of right ventricular function in patients with idiopathic pulmonary arterial hypertension. *Int J Cardiol* 2010;140(3):272–278.
99. Kassem E, Humpl T, Friedberg MK. Prognostic significance of 2-dimensional, M-mode, and Doppler echo indices of right ventricular function in children with pulmonary arterial hypertension. *Am Heart J* 2013;165(6):1024–1031.
100. Berman GO, Reichel N, Brownson D, Douglas PS. Effects of sample volume location, imaging view, heart rate and age on tricuspid velocimetry in normal subjects. *Am J Cardiol* 1990;65(15):1026–1030.
101. Sallach JA, Tang WH, Borowski AG, Tong W, Porter T, Martin MG, Jasper SE, Shrestha K, Troughton RW, Klein AL. Right atrial volume index in chronic systolic heart failure and prognosis. *JACC Cardiovasc Imaging* 2009;2(5):527–534.
102. Yates AR, Welty SE, Gest AL, Cua CL. Myocardial tissue Doppler changes in patients with bronchopulmonary dysplasia. *J Pediatr* 2008;152(6):766–770.
103. Okumura K, Slorach C, Mroczek D, Dragulescu A, Mertens L, Redington AN, Friedberg MK. Right ventricular diastolic performance in children with pulmonary arterial hypertension associated with congenital heart disease: correlation of echocardiographic parameters with invasive reference standards by high-fidelity micromanometer catheter. *Circ Cardiovasc Imaging* 2014;7(3):491–501.
104. Pye MP, Pringle SD, Cobbe SM. Reference values and reproducibility of Doppler echocardiography in the assessment of the tricuspid valve and right ventricular diastolic function in normal subjects. *Am J Cardiol* 1991;67(4):269–273.
105. Nagaya N, Satoh T, Uematsu M, Okano Y, Kyotani S, Nakanishi N, Kunieda T. Shortening of Doppler-derived deceleration time of early diastolic transmitral flow in the presence of pulmonary hypertension through ventricular interaction. *Am J Cardiol* 1997;79(11):1502–1506.

106. Schiller NB, Shah PM, Crawford M, DeMaria A, Devereux R, Feigenbaum H, Gutgesell H, et al. Recommendations for quantitation of the left ventricle by two-dimensional echocardiography. *J Am Soc Echocardiogr* 1989;2(5):358–367.
107. Chuang ML, Hibberd MG, Salton CJ, Beaudin RA, Riley MF, Parker RA, Douglas PS, Manning WJ. Importance of imaging method over imaging modality in noninvasive determination of left ventricular volumes and ejection fraction: assessment by two- and three-dimensional echocardiography and magnetic resonance imaging. *J Am Coll Cardiol* 2000;35(2):477–484.
108. Koestenberger M, Nagel B, Ravekes W, Avian A, Burmas A, Grangl G, Cvirn G, Gamillscheg A. Reference values and calculation of z-scores of echocardiographic measurements of the normal pediatric right ventricle. *Am J Cardiol* 2014;114(10):1590–1598.
109. Cantinotti M, Scalese M, Murzi B, Assanta N, Spadoni I, De Lucia V, Crocetti M, et al. Echocardiographic nomograms for chamber diameters and areas in Caucasian children. *J Am Soc Echocardiogr* 2014;27(12):1279–1292.
110. Bustamante-Labarta M, Perrone S, de la Fuente RL, Stutzbach P, de la Hoz RP, Torino A, Favalaro R. Right atrial size and tricuspid regurgitation severity predict mortality or transplantation in primary pulmonary hypertension. *J Am Soc Echocardiogr* 2002;15(10):1160–1164.
111. Habib G, Torbicki A. The role of echocardiography in the diagnosis and management of patients with pulmonary hypertension. *Eur Respir Rev* 2010;19(118):288–299. doi:10.1183/09059180.00008110.
112. Cioffi G, de Simone G, Mureddu G, Tarantini L, Stefanelli C. Right atrial size and function in patients with pulmonary hypertension associated with disorders of respiratory system or hypoxemia. *Eur J Echocardiogr* 2007;8(5):322–331.
113. Brennan JM, Blair JE, Goonewardena S, Ronan A, Shah D, Vasaiwala S, Kirkpatrick JN, Spencer KT. Reappraisal of the use of inferior vena cava for estimating right atrial pressure. *J Am Soc Echocardiogr* 2007;20(7):857–861.
114. Kircher BJ, Himelman RB, Schiller NB. Noninvasive estimation of right atrial pressure from the inspiratory collapse of the inferior vena cava. *Am J Cardiol* 1990;66(4):493–496.
115. Beigel R, Cercek B, Luo H, Siegel RJ. Noninvasive evaluation of right atrial pressure. *J Am Soc Echocardiogr* 2013;26(9):1033–1042.
116. Takahashi K, Inage A, Rebeyka IM, Ross DB, Thompson RB, Mackie AS, Smallhorn JF. Real-time 3-dimensional echocardiography provides new insight into mechanisms of tricuspid valve regurgitation in patients with hypoplastic left heart syndrome. *Circulation* 2009;120(12):1091–1098.
117. Dragulescu A, Grosse-Wortmann L, Fackoury C, Riffle S, Waiss M, Jaeggi E, Yoo SJ, Friedberg MK, Mertens L. Echocardiographic assessment of right ventricular volumes after surgical repair of tetralogy of Fallot: clinical validation of a new echocardiographic method. *J Am Soc Echocardiogr* 2011;24(11):1191–1198.
118. Renella P, Marx GR, Zhou J, Gauvreau K, Geva T. Feasibility and reproducibility of three-dimensional echocardiographic assessment of right ventricular size and function in pediatric patients. *J Am Soc Echocardiogr* 2014;27(8):903–910.
119. Grewal J, Majdalany D, Syed I, Pellikka P, Warnes CA. Three-dimensional echocardiographic assessment of right ventricular volume and function in adult patients with congenital heart disease: comparison with magnetic resonance imaging. *J Am Soc Echocardiogr* 2010;23(2):127–133.
120. Leibundgut G, Rohner A, Grize L, Bernheim A, Kessel-Schaefer A, Bremerich J, Zellweger M, Buser P, Handke M. Dynamic assessment of right ventricular volumes and function by real-time three-dimensional echocardiography: a comparison study with magnetic resonance imaging in 100 adult patients. *J Am Soc Echocardiogr* 2010;23(2):116–126.
121. Van der Zwaan HB, Helbing WA, McGhie JS, Geleijnse ML, Luijnenburg SE, Roos-Hesselink JW, Meijboom FJ. Clinical value of realtime three-dimensional echocardiography for right ventricular quantification in congenital heart disease: validation with cardiac magnetic resonance imaging. *J Am Soc Echocardiogr* 2010;23(2):134–140.
122. Kong D, Shu X, Dong L, Pan C, Cheng L, Yao H, Zhou D. Right ventricular regional systolic function and dyssynchrony in patients with pulmonary hypertension evaluated by three-dimensional echocardiography. *J Am Soc Echocardiogr* 2013;26(6):649–656.
123. Tamborini G, Marsan NA, Gripari P, Maffessanti F, Brusoni D, Muratori M, Caiani EG, Fiorentini C, Pepi M. Reference values for right ventricular volumes and ejection fraction with real-time three-dimensional echocardiography: evaluation in a large series of normal subjects. *J Am Soc Echocardiogr* 2010;23(2):109–115.
124. van der Zwaan HB, Geleijnse ML, McGhie JS, Boersma E, Helbing WA, Meijboom FJ, Roos-Hesselink JW. Right ventricular quantification in clinical practice: two-dimensional vs. three-dimensional echocardiography compared with cardiac magnetic resonance imaging. *Eur J Echocardiogr* 2011;12(9):656–664.
125. Grapsa J, O'Regan DP, Pavlopoulos H, Durighel G, Dawson D, Nihoyannopoulos P. Right ventricular remodelling in pulmonary arterial hypertension with three-dimensional echocardiography: comparison with cardiac magnetic resonance imaging. *Eur J Echocardiogr* 2010;11(1):64–73.
126. Grapsa J, Gibbs JS, Dawson D, Watson G, Patni R, Athanasiou T, Punjabi PP, Howard LS, Nihoyannopoulos P. Morphologic and functional remodeling of the right ventricle in pulmonary hypertension by real time three dimensional echocardiography. *Am J Cardiol* 2012; 109(6):906–913.
127. Lu X, Nadvoretzkiy V, Bu L, Stolpen A, Ayres N, Pignatelli RH, Kovalchin JP, Grenier M, Klas B, Ge S. Accuracy and reproducibility of real-time three-dimensional echocardiography for assessment of right ventricular volumes and ejection fraction in children. *J Am Soc Echocardiogr* 2008;21(1):84–89.
128. Friedberg MK, Su X, Tworetzky W, Soriano BD, Powell AJ, Marx GR. Validation of 3D echocardiographic assessment of left ventricular volumes, mass, and ejection fraction in neonates and infants with congenital heart disease: a comparison study with cardiac MRI. *Circ Cardiovasc Imaging* 2010;3(6):735–742.
129. Khoo NS, Young A, Occleshaw C, Cowan B, Zeng IS, Gentles TL. Assessments of right ventricular volume and function using three-dimensional echocardiography in older children and adults with congenital heart disease: comparison with cardiac magnetic resonance imaging. *J Am Soc Echocardiogr* 2009;22(11):1279–1288.
130. Li Y, Wang Y, Zhai Z, Guo X, Yang Y, Lu X. Real-time three-dimensional echocardiography to assess right ventricle function in patients with pulmonary hypertension. *PLoS ONE* 2015;10:e0129557. doi:10.1371/journal.pone.0129557.
131. Hansmann G, Hoeper MM. Registries for paediatric pulmonary hypertension. *Eur Respir J* 2013;42(3):580–583.
132. Taylor C, Derrick G, McEwan A, Haworth S, Sury M. Risk of cardiac catheterization under anaesthesia in children with pulmonary hypertension. *Br J Anaesth* 2007;98(5):657–661.
133. Baldi F, Fuso L, Arrighi E, Valente S. Optimal management of pulmonary arterial hypertension: prognostic indicators to determine treatment course. *Ther Clin Risk Manag* 2014;10:825–839.
134. Adatia I, Haworth S, Wegner M, Barst R, Ivy D, Stenmark K, Karkowsky A, Rosenzweig E, Aguilar C. Clinical trials in neonates and children: report of the pulmonary hypertension academic research consortium pediatric advisory committee. *Pulm Circ* 2013;3(1):252–266.
135. Vonk-Noordegraaf A, Westerhof N. Describing right ventricular function. *Eur Respir J* 2013;41(6):1419–1423.
136. Vanderpool RR, Pinsky MR, Naeije R, Deible C, Kosaraju V, Bunner C, Mathier MA, Lacomis J, Champion HC, Simon MA. RV-pulmonary arterial coupling predicts outcome in patients referred for pulmonary hypertension. *Heart* 2015;101(1):37–43.
137. Ernande L, Cottin V, Leroux PY, Girerd N, Huez S, Mulliez A, Bergerot C, et al. Right isovolumic contraction velocity predicts survival in pulmonary hypertension. *J Am Soc Echocardiogr* 2013;26(3): 297–306.